PROCEEDINGS, 45th Workshop on Geothermal Reservoir Engineering
Stanford University, Stanford, California, February 10-12, 2020
SGP-TR-216

Production Chemistry Evidence for an EGS-type Reservoir in Roosevelt Hot Springs and Implications for Utah FORGE

Stuart F. Simmons[1,2], Stefan Kirby[3], Rick Allis[3], and Joe Moore[1]

[1]EGI, University of Utah, 423 Wakara Way, Ste 300, Salt Lake City, UT
[2]Department of Chemical Engineering, University of Utah, 50 S. Central Campus Dr., Salt Lake City, UT 84112
[3]Utah Geological Survey, 1594 W. North Temple St., Salt Lake City, UT 84114

ssimmons@egi.utah.edu

Keywords: EGS heat exchange, reservoir fluid geochemistry, production changes, injection breakthrough, Roosevelt Hot Springs

ABSTRACT

The Roosevelt Hot Springs hydrothermal system is a Basin and Range-type geothermal resource located at the base of the Mineral Mountains in southwestern Utah, 4 km east of the Utah FORGE EGS site. Exploration drilling down to 2000 m depth in the 1970s proved the existence of a hot water hydrothermal plume that covers ~3 km^2. The conventional reservoir is made of fractured Oligocene-Miocene granitoid rock that in terms of rock type and properties is analogous to the Utah FORGE EGS reservoir.

Since 1984, the Blundell power plant has been in continuous production, obtaining fluid supply (240-290 kg/s) from four wells with feed point temperatures of 240° to 265° C. A nearby deep well (14-2) has been used for long term but variable injection that represents between 25 and 70% of the total injectate.

Time series analysis of production fluid chemistry including pre-production, 1991-1992, 2015 and 2016, provide clear evidence of injection breakthrough as represented by increases in chloride and modest drops in enthalpy early in the production history. Taking into account continuous steam loss and mixing effects, simple models show that EGS type heat extraction has been significant and helped to sustain reservoir productivity for at least 25 years.

We infer from the surface geology that sub-vertical fracture-related permeability in the reservoir forms baffles that facilitate fluid flow and heat exchange as the injectate migrates into the production zone. These results show the promise of developing an EGS reservoir at the Utah FORGE site.

1. INTRODUCTION

Utah FORGE is located in the north Milford valley, approximately 4 km west of Roosevelt Hot Springs, which is a high temperature geothermal resource that has been in continuous production since 1984 (Fig. 1). Both areas share a similar geology. More relevant is that the development and production history of the conventional geothermal resource at Roosevelt Hot Springs provides useful information in respect to EGS reservoir development and management at the Utah FORGE site. This paper specifically looks at the evidence for EGS-type heat transfer in Roosevelt Hot Springs reservoir since the start of production.

Roosevelt Hot Springs has an elongate-shaped production field, which covers an area ~3 km^2 and which is situated east of and subparallel to the Opal Mound fault. Roosevelt Hot Springs is the largest of the three relatively closely spaced producing geothermal fields in southwestern Utah, and it is one of the few geothermal systems in the western USA to be entirely hosted by fractured crystalline rock. This host rock is made of Oligocene-Miocene age granitoid, which intruded Precambrian gneiss and schist (e.g. Capuano and Cole, 1982; Nielson et al., 1986; Coleman and Walker, 1992; Simmons et al., 2019). Modern hydrothermal activity appears to be associated with recent magmatism that produced rhyolitic flow dome complexes (0.8 to 0.5 Ma), which includes Bailey Ridge located only 2-3 km east of the steam field (Lipman et al., 1978; Moore and Nielson, 1994). Exploration drilling (1975-1984) proved a maximum reservoir temperature of ~265°C at >600 m depth (Faulder, 1991, 1994; Allis and Larsen, 2012). Production commenced in 1984, with the commissioning of the Blundell flash plant (23MWe net single-stage). Additional generation was commissioned in 2008 in the form of a bottom cycle binary plant (10 MWe net).

Capuano and Cole (1982) provided the first description and interpretation of reservoir fluid chemistry and fluid-mineral equilibria based on data collected before full scale field production commenced. In the intervening years, information regarding production-induced effects have been limited to physical parameters, including temperature and pressure (Faulder, 1991; 1994; Yearsley, 1994; Allis and Larsen, 2012). In 2018, updated information on the production fluid chemistry through 2016 was reported in order to document the reservoir response to production (Simmons et al., 2018). These data are reviewed below, especially the chloride-enthalpy trends, which evolved over time in response to more than 30 years of sustained geothermal energy production.

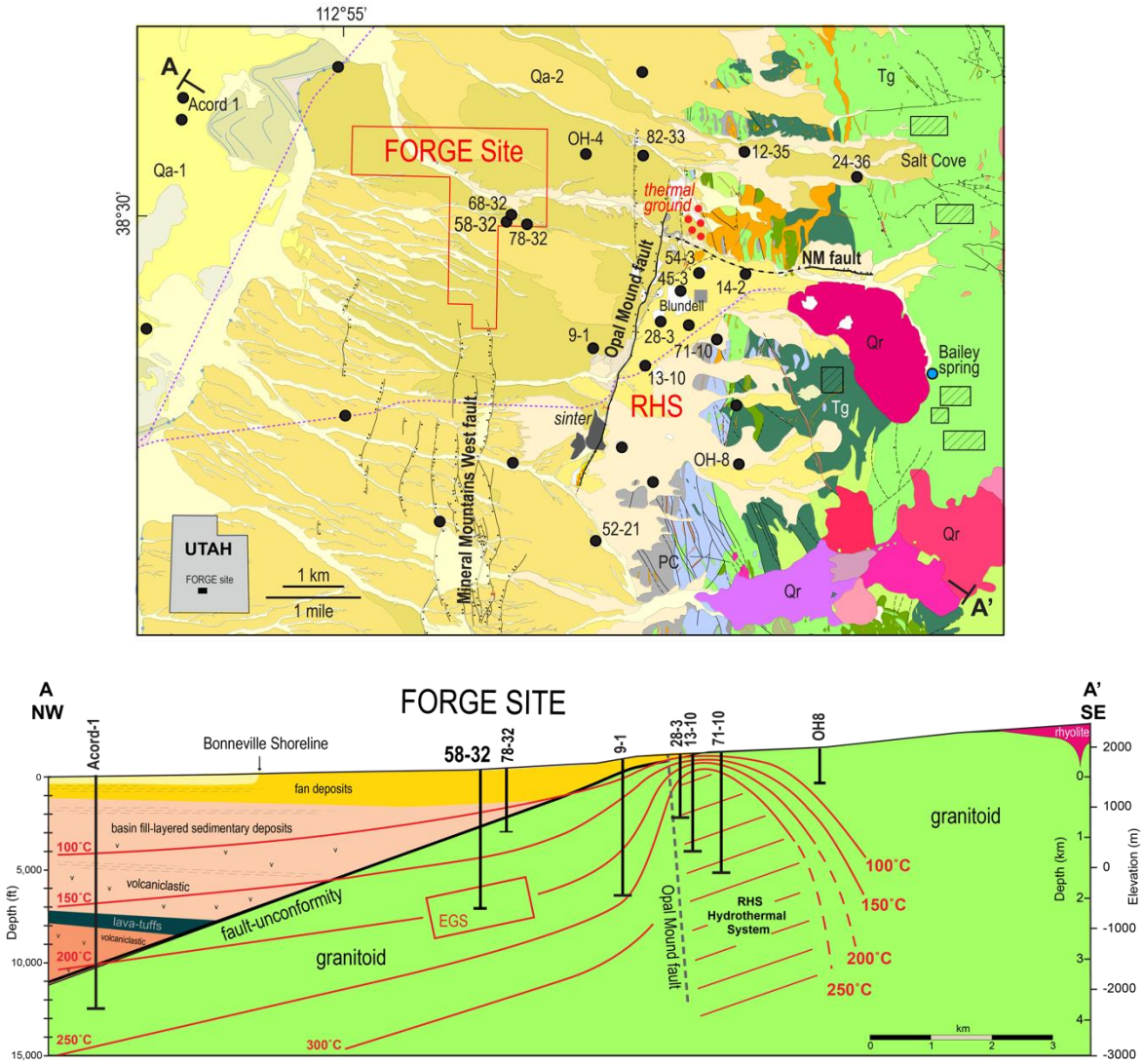

Figure 1: Geological map and cross section for Roosevelt Hot Springs (RHS) and the Utah FORGE site based on the compilation of new field observations, well data, and previous work (Nielson et al., 1986; Kirby, 2019). The rhyolite flow (red) west of Bailey spring makes up Bailey Ridge. Abbreviations: Qa-1=Lake Bonneville silts and sands; Qa-2=alluvial fan deposits; Qr=Quaternary rhyolite lava and pyroclastic deposits; Tg=Tertiary granitoid; PC=Precambrian gneiss; black filled circles=wells. In cross section, the red box represents approximate position of the Utah FORGE EGS reservoir.

2. GEOTHERMAL FLUID PRODUCTION AND INJECTION

Since 1984, the Blundell power plant has been in continuous production, obtaining fluid supply (240-290 kg/s) from four wells with feed point temperatures of 240° to 265° C. A nearby deep well (14-2) has been used for long term but variable injection that represents between 25 and 70% of the total injectate. Reservoir permeability is inferred to be controlled by a zone of interconnected fractures in granitic host rocks directly east of the Opal Mound fault (Nielson et al., 1986; Faulder, 1991). For at least the first ten years, the total fluid production supplied approximately 50 kg/s steam and 240 kg/s water that was separated near the wellhead by cyclone separators at 9-11 bars absolute (Yearsley, 1994; Allis and Larsen, 2012). In 2015 and 2016 when the production fluids were sampled, the total two-phase fluid production had dropped slightly with separation pressures of 8-9 bars. In the natural preproduction state, the deep upflow of fluid was approximately 60 kg/s (Allis et al., 2018).

After separating steam from the produced two-phase fluid for power generation, the residual water is injected into the subsurface. From 1984 to 1991, water was injected into just two wells 14-2 and 82-33. A third well, 12-35, was added in 1991, and all three injectors have been in continuous use ever since. Although 14-2 was hot and productive, it has always been used as an injector, taking roughly between 40 and 70% of the total injectate between 1984 and 2008. By 2014 and 2015, only 25-40 % of the total injectate went into 14-2.

Geothermal fluid production induced physical changes, including a precipitous drop in pressure of up to 30-35 bars that occurred over the first four years of production (Yearsley, 1994; Allis and Larsen, 2012). At the same time, the piezometric level dropped by 250-300 m, forming a shallow steam zone (Yearsley, 1994) and the modern-day steaming ground near the intersection of Opal Mound and NM faults. From the mid-1990s onward, the pressure and temperature continued to decline but much more gradually. By 2010, most of the wells displayed a total drop in pressure of nearly 40 bars from preproduction conditions, the only exception being well 54-3, which had dropped only 17 bars, presumably as a result of pressure support from injection into nearby well 14-2 (Allis and Larsen, 2012). The decline in pressure across the production field was accompanied by decrease in subsurface temperatures of about 10-15° C. For example, downhole measurements in 54-3 show the maximum temperature cooled from the initial condition of 265° C to 245° C by 2012 (Fig. 2).

3. PRODUCTION CHEMISTRY

Chemical data were acquired on samples collected from all four production wells in 2015 and 2016 (Simmons et al., 2018). To make these analytical results useful, the values were recalculated to reservoir conditions, assuming fluid entered the well at a deep level and as a single-phase liquid, and by using heat and mass balance expressions, well enthalpies and sampling pressures (Henley et al., 1984). The enthalpies determined from chemical geothermometers and down hole temperature measurements gives consistent results (Simmons et al., 2018).

In general, the production fluid compositions are similar to those at the start of reservoir exploitation, having near neutral pH, total dissolved solids of 7000-10,000 mg/kg, and ionic ratios of Cl/HCO_3 ~50-100, Cl/SO_4 ~50-100, and Na/K ~4-5. The quartz-silica equilibrium temperatures range from 240 to 260°C, whereas the Na-K equilibration temperatures range from 270 to 310°C, which conceivably reflects thermal conditions in the deep part (>3 km?) of the upflow zone. The H_2/Ar and CO_2/Ar geothermometers give equilibration temperatures of 190-310°C. The helium isotope R/Ra values of 2.1 to 2.2 and N_2-Ar-He data imply derivation from a deep mafic magmatic source.

4. CHLORIDE-ENTHALPY TRENDS

The heat and mass transfer effects induced by production are reflected in the chloride and enthalpy trends (Fig. 3). Before production began, the reservoir fluid had a chloride composition of 3000-3500 mg/kg and an enthalpy of 1050 to 1160 kJ/kg. Wells 14-2 and 54-3 represent the hottest and least diluted liquid in the reservoir, corresponding to the central upflow zone of the system, whereas 72-16, having cooler enthalpy, is closer to the periphery of the upflow zone (Capuano and Cole, 1982).

By 1992, the reservoir fluid composition is modified, mostly by inmixing of injectate from 14-2, which has a low enthalpy and a high chloride concentration compared to the original deep upflow water. This effect is observed in the change in 54-3 to higher chloride and lower enthalpy. Data for 13-10, 28-3, and 45-3 first appear in this time period, and the chloride concentration of the injected water is deduced based on the amount of steam produced for each well. By 2008, the chloride concentration of the injectate had risen to ~4800 mg/kg, based on an analysis of a sample obtained from the inlet of the newly commissioned binary plant (Pacificorp unpublished data). Exiting the binary plant, the liquid enthalpy was reduced to 400 kJ/kg before being injected into the subsurface.

The 2015-2016 datasets show continued increase in chloride accompanied by minor decrease in enthalpy. These effects reflect the inmixing of injectate from 14-2. Notably and going southward, wells 54-3, 45-3 and 28-3, show progressively decreasing concentrations of chloride coinciding with increasing distance from 14-2. The least modified reservoir water is represented by 13-10, with the first measurable increase in chloride and decrease in enthalpy being detected between 2015 and 2016; the maximum measured temperature in this well dropped from 264 to 248°C between 1989 and 1999 (Allis and Larsen, 2012).

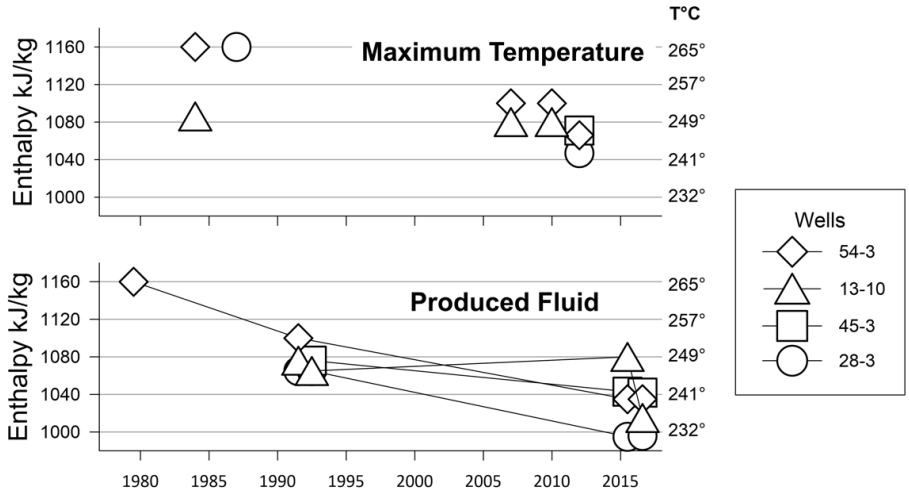

Figure 2. Temperature and enthalpy trends in production wells showing the gradual cooling of the reservoir with time. The top graph shows the maximum temperatures measured in wells based on downhole temperature surveys (Allis and Larsen,

2012). The bottom graph shows the enthalpies of flowing hot water and steam at the wellheads except for 54-3 in 2015-2016, which were corrected for excess steam supply (Simmons et al., 2018).

The wellhead enthalpies of 54-3 in 2015 and 2016 show that the fluid feeding this well comprised a two-phase mixture of steam and liquid. Although the precise cause of this development is difficult to pin down, it probably represents enhanced steam production associated with a localized fracture-controlled pressure drop. The most recent downhole temperature measurement in 2012 confirms that the deep fluid entering the well had cooled to 245°C (Fig. 2). In addition, the evaluation of silica geothermometry suggests that the steam fractions for produced fluids declined from 0.155 to 0.1 between 2015 and 2016 (Fig. 3). Using this information to correct the overall time series trend for well 54-3 gives a result that closely resembles the trend for well 45-3 (Figs. 2 and 3).

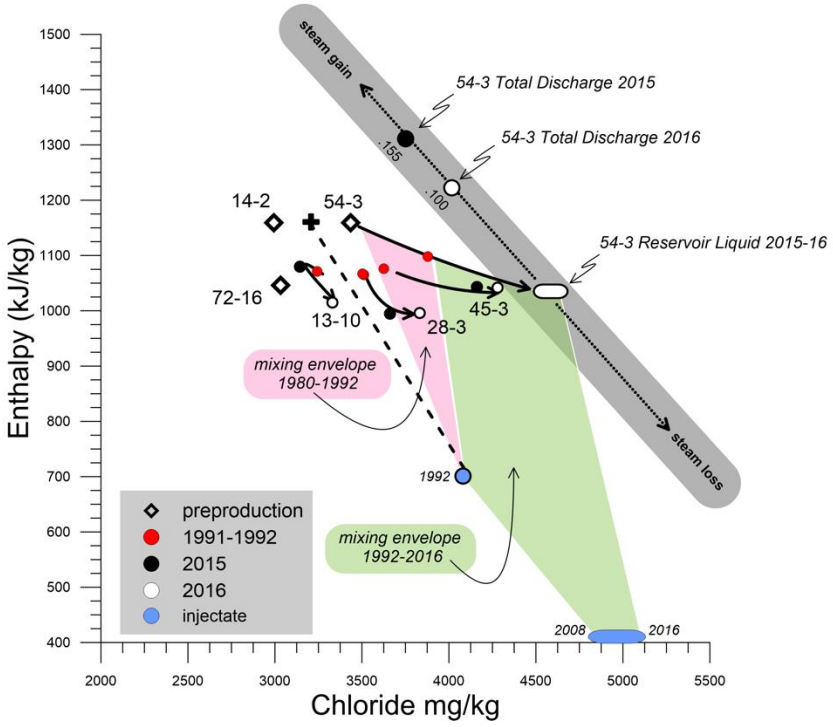

Figure 3. Chloride-enthalpy plot showing the evolution of production fluids in response to injection, mixing, and boiling. The 1991-1992 production and injectate fluid compositions come from an internal report by Intermountain Geothermal Company. Grey bold line represents the trend for steam-loss and steam gain. The diagonal dashed line represents the mixing trend model between a reservoir water at the start of production (i.e., 3200 mg/kg Cl, 1160 kJ/kg) and injectate (4120 mg/kg Cl, 700 kJ/kg).

5. MODEL CALCULATIONS

In order to quantify how much injectate mixed with reservoir water to cause the increase in produced chloride water concentration, a simple two-component model is set up based on an arithmetic series of chloride and heat balance calculations using the following expressions:

$$Cl_{reservoir} = aCl_{reservoir\ (n-1)} + bCl_{injectate} \quad (1)$$

$$H_{reservoir} = aH_{reservoir\ (n-1)} + bH_{injectate} \quad (2)$$

$$Cl_{injectate} = Cl_{reservoir\ (n-1)} / (1-y_{(n-1)}) \quad (3)$$

$$y_{(n-1)} = (H_{reservoir\ (n-1)} - H_{injectate}) / H_{evaporation} \quad (4)$$

Where $Cl_{reservoir}$ is the reservoir chloride concentration of the mixed water entering the well, $Cl_{reservoir\ (n-1)}$ is the chloride concentration in reservoir liquid entering the well in the preceding step, $Cl_{injectate}$ is the chloride concentration based on steam loss from the produced fluid represented by $Cl_{reservoir\ (n-1)}$, $y_{(n-1)}$ is the mass fraction of steam removed from produced fluid at the surface, $H_{reservoir}$ is the reservoir enthalpy of the mixed water, $H_{reservoir\ (n-1)}$ is the reservoir enthalpy in the preceding interval, and $H_{injectate}$ and $H_{evaporation}$ are fixed at 700 kJ/kg and 2065 kJ/kg, respectively, based on vapor-saturation and steam separation at 7 bar. The mass fractions of reservoir water and injectate in the mixed fluid are represented by *a* and *b*, respectively. The aim of the modeling is directed at replicating the effects of

steam-loss and mixing between a single producer well and a single injector well as represented by wells 45-3 (or 54-3), and well 14-2, respectively.

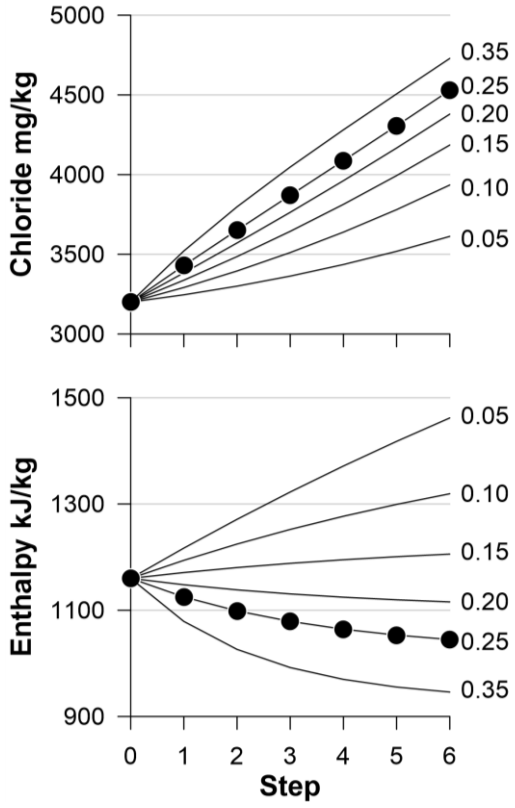

Figure 4. Model calculations of the evolution of reservoir chloride concentration and enthalpy of geothermal water feeding a production well based on a two-component mixing model and constant heat sweep of 320 kJ/kg by the injectate. The time step is dimensionless. Line labels indicate the fraction of injectate mixed with reservoir water, and black filled circles indicate model path that best fits time series evolution of well 45-3.

A number of run calculations were made to determine how successive slugs of injectate enrich the chloride concentration and reduce the enthalpy of the produced water entering the well in a step-wise manner over time. In each run, the mass fractions of the two components (reservoir water and injectate) are held constant, and the starting value of the reservoir chloride is 3200 mg/kg and the starting value of the reservoir enthalpy is 1160 kJ/kg. Each step (n) represents an arbitrary time interval of mixing between the evolving reservoir water and the evolving injectate composition. This liquid is then flashed to reflect ascent in the production well, with the fraction of steam that forms being separated at the surface, causing the liquid to increase in chloride concentration and a decrease in enthalpy. This separated liquid becomes the injectate for the next step in mixing. The results of these calculations trace the straight dashed line in Figure 3, which terminates at an injectate composition of 4120 mg/kg Cl, irrespective of the mass proportions of reservoir liquid and injectate in the mixed fluid. It is clear that the simple mixing model cannot possibly account for the chloride-enthalpy trends with time, and the breakthrough of injectate must be accompanied by a significant amount of heat sweep between well 14-2 and the feed points in production wells.

A second set of run calculations were made on the same premise as the first set, but with addition of a fixed quantity of supplementary heat to each reservoir mixture. No input of deep chloride water is considered. For example, the results of adding 80 kJ/kg heat are shown in Figure 4. In all the runs, the chloride concentration increases over time, but only for mass fractions of injectate of 0.2 and greater do the enthalpy trends decrease over time. The model run that best matches the trends for 45-3 and 54-3 are given by an injectate mass fraction of 0.25 (Figs. 4 and 5), which equates to 320 kJ/kg of heat sweep between the injector and the producer assuming the injectate introduces all the new heat. Adjustments to the amount of added heat were tested, but few of the resulting chloride-enthalpy trends matched the histories of 45-3 or 54-3 (Fig. 5), and of these, they were all within ~20%. By simultaneously evaluating both chloride and enthalpy a relatively narrow range of apparently valid model results were obtained. From comparison of the model and time series evolution in chloride and enthalpy (Fig. 5), the interval of the time step (n) is 5.3 years.

A third set of model runs were calculated in which a three-component mixing model was assessed. In these, a fraction of preproduction chloride water was added to the reservoir fluid to produce a mixture of injectate, deep upflow, and existing reservoir water, along with 80 kJ/kg of heat. Just as in the previous case, the added heat is essential to matching the enthalpy-chloride trends in Figure 3. The

proportion of injectate to deep upflow is held constant at 2:1, and the best match was obtained for a fluid made of 60% reservoir water, 27% injectate, and 13% deep upflow. Assuming again that all the new heat is introduced by the injectate indicates 296 kJ/kg of heat sweep between the injector and producer.

The preceding mixing models are simplistic in which the proportions of end-member fluids are held constant and the steam fraction of produced fluid is modified by modest cooling. Furthermore, variation in the flow rate injected into 14-2 is not considered. Some of the results closely match the enthalpy-chloride trends in Figures 3 and 5, and these indicate supplementary heat is gained by the reservoir fluid, which is presumed to be introduced by the injectate as it heats up and flows back into the reservoir. The amount of heating is roughly 300 to 320 kJ/kg. Mass flows and heat sweep are assumed to be unchanging, even though they are more likely to be variable and incorporate non-linear effects as fluid migrates through fractured rock media. In the three-component mixing model, the deep upflow composition is assumed to have the same chloride concentration and enthalpy as the preproduction reservoir fluid, and there are no modern data to better constrain these values. Lastly, the injectate enthalpy is held constant at 700 kJ/kg, but in 2008 this declined to ~400 kJ/kg with the commissioning of the binary plant.

Keeping in mind all the caveats in the preceding paragraph, the results shown in Figures 4 and 5 can be used to further estimate the thermal power production in wells 54-3 and 45-3 associated with heated injectate from 14-2. In 2015-2016, the combined fluid production from the two wells was 140-145 kg/s, 25% of which appears to be represented by injectate. Taking the injectate contribution to be 35 kg/s and the added heat to be 300 kJ/kg based on the 700 kJ/kg cutoff, the contribution of thermal power is about 10 MW, but using a lower cutoff value of 400 kJ/kg this doubles to 20 MW. Over a thirty-year period this equates to a minimum of $3x10^{11}$ kJ of heat sweep. The validity of these calculations needs to be checked against results of numerical reservoir modeling. The values nonetheless help to quantify the amount of heat gained by injection and production of geothermal fluid.

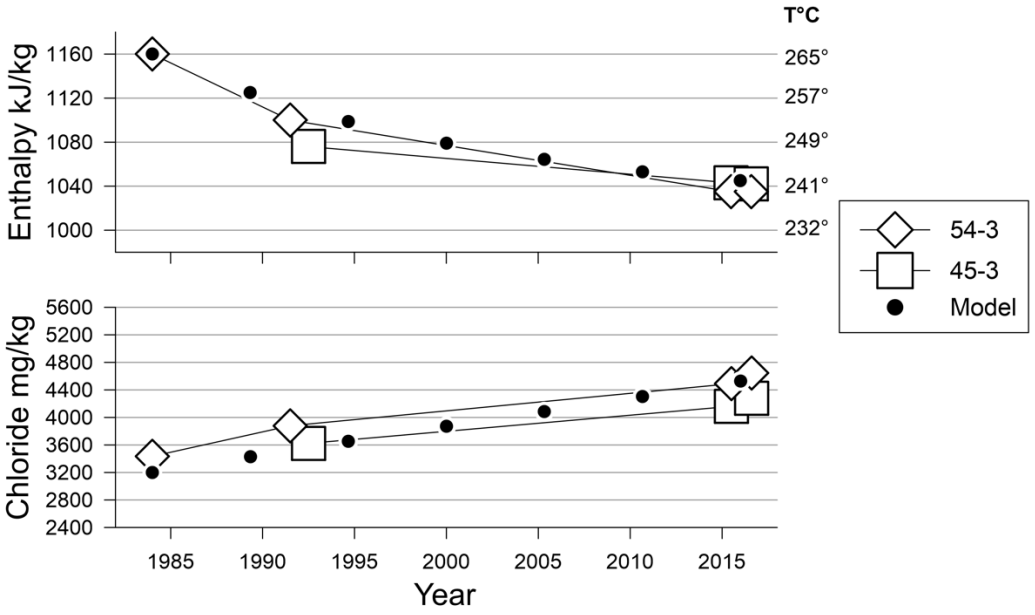

Figure 5. Comparison of the time series evolution of production enthalpies and chlorides for wells 54-3 and 45-3 with the model calculations (0.25 injection fraction) shown in Figure 4.

6. CONCLUSIONS

The production chemistry data and downhole temperature measurements at Roosevelt Hot Springs provide snapshots of reservoir evolution in response to production and injection between 1984 and 2016. The temporal and spatial chloride-enthalpy patterns show how injectate spread westward and southward through the reservoir, only just reaching the most distal well, 13-10, by 2016 (Fig. 3). Simplistic mixing models also show that geothermal energy production could not have been sustained without EGS-type conductive heating of injectate, across multiple fracture surfaces, as the injectate moved from 14-2 into the production reservoir.

The model calculations suggest a gradual increase in chloride and decrease in enthalpy associated with injection breakthrough, which appears to have initiated soon after production commenced and then continued at a similar rate for more than 30 years. We infer from the surface geology that sub-vertical fracture-related permeability in the reservoir forms baffles which facilitate both fluid flow and heat exchange as the injectate migrates into the production zone. Unfortunately, the geometry of the fracture network and its surface area, along with rates of fluid flow and water-rock heat exchange are difficult to characterize. In this respect, tracer injection testing would be worthwhile. Despite these limitations, estimates of heat transfer are around 300 to 320 kJ/kg injectate, and these are minimum values that do not include compensation for the thermal energy extracted for the binary plant since 2008. Clearly, heated injectate has made

significant contribution to the total energy production within a conventional geothermal resource. These results show the promise of developing an EGS reservoir at the Utah FORGE site.

7. ACKNOWLEDGMENTS

This work is sponsored by the DOE EERE Geothermal Technologies Office project DE-EE0007080 Enhanced Geothermal System Concept Testing and Development at the Milford City, Utah FORGE Site. Special thanks are extended to PacificCorp for permission and assistance with the sampling of production fluids.

REFERENCES

Allis, R. G. and Larsen, G.: Roosevelt Hot Springs Geothermal field, Utah – reservoir response after more than 25 years of power production, *Proceedings*. 37th Workshop on Geothermal Reservoir Engineering, Stanford University, Stanford, CA, (2012).

Allis, R.G., Gwynn, M., Hardwick, C., Hurlbut, W., and Moore, J.N.: Thermal characteristics of the FORGE site, Milford, Utah, *Transactions,* Geothermal Resources Council Transactions, **42** (2018), 15 p.

Capuano, R. M., and Cole, D. R.: Fluid-mineral equilibria in a hydrothermal system, *Geochimica Cosmochimica Acta*, **46** (1982), 1353-1364.

Coleman, D.S., and Walker, J.D.: Evidence for the generation of juvenile granitic crust during continental extension, Mineral Mountains batholith, Utah, *Journal of Geophysical Research*, **97** (1992), 11011-11024.

Faulder, D.D.: Conceptual geologic model and native state of the Roosevelt Hot Springs hydrothermal system, *Proceedings* of the 16th Workshop on Geothermal Reservoir Engineering, Stanford University (1991), 131-142.

Faulder, D.D.: Long-term flow test #1, Roosevelt Hot Springs, Utah, *Transactions,* Geothermal Resources Council Transactions, **18** (1994), 583-590.

Henley, R.W., Truesdell, A.H., and Barton, P.B. Jr.: Fluid-mineral equilibria in hydrothermal systems, *Reviews in Economic Geology,* **1** (1984), 267 p.

Kirby, S.: Revised mapping of bedrock geology adjoining the Utah FORGE site, *Miscellaneous Publication 169-A*, Utah Geological Survey (2019*).*

Lipman, P.W., Rowley, P.D., Mehnert, H.H., Evans, S.H., Jr., Nash, W.P., and Brown, F.H.: Pleistocene rhyolite of the mineral mountains, Utah: geothermal and archeological significance, *US Geological Survey Journal of Research*, **6** (1978), 133-147.

Moore, J.N., and Nielsen, D.L.: An overview of geology and geochemistry of the Roosevelt Hot Springs geothermal area, *Utah Geological Association Publication* **23** (1994), 25–36.

Nielson, D. L., Evans, S.H., and Sibbett, B.S.: Magmatic, structural, and hydrothermal evolution of the Mineral Mountains intrusive complex, Utah, *Geological Society of America Bulletin*, **97** (1986), 765-777.

Simmons, S.F., Kirby, S., Allis, R., Moore, J.N., and Fischer, T.: 2018, Update on the production chemistry of Roosevelt Hot Springs reservoir, *Proceedings*, 43rd Workshop on Geothermal Reservoir Engineering, Stanford University, Stanford, CA (2018).

Simmons, S. F., Kirby, S., Bartley, J., Allis, R., Kleber, E., Knudsen, T., Miller, J., Hardwick, C., Rahilly, K., Fischer, T., Jones, C., and Moore, J.N.: Update on the geoscientific understanding of the Utah FORGE site, *Proceedings*, 44th Workshop on Geothermal Reservoir Engineering, Stanford University, Stanford, CA (2019).

Yearsley, E.: Roosevelt Hot Springs reservoir model applied to forecasting remaining field potential, *Proceedings* Geothermal Resources Council, **18** (1994), 617-622.